Supporting Information

Yao et al. 10.1073/pnas.0912988107

SI Text

EDX. Spatially specific EDX data on the cross section of the *C. squamiferum* shell is provided in Fig. S1.

XRD. X-ray diffraction data on the shell of *C. squamiferum* is provided in Fig. S2.

Advantages of Heterogeneous Interfacial Geometries. Another interesting feature is the heterogeneous wavy interfacial geometry of the OL/ML, which was approximated in a modified multilayered finite element analysis (FEA) simulation and compared to a simulation containing a flat OL/ML interface. The wavy interfacial geometry did not have a significant effect on the overall inelastic energy dissipation, radial displacement, or bending stiffness of the entire exoskeletal structure; displacement of the indenter into the ML; or the local stress distributions in the underlying layers due to its small thickness in the overall geometry (Fig. S3). However, dramatically different discontinuous stress distributions were observed for the wavy interface within the OL itself and along the OL/ML interface compared to the flat OL/ML interface, with spatially distinct regions of high tensile and compressive normal stresses (S_{33}) and of high and low shear stress (S_{23}). Regions of high tensile S_{33} and high S_{23} provide susceptibility to interfacial delamination, which if initiated would subsequently be arrested by neighboring regions of interfacial compression and low shear (1). Localized interfacial delamination was, in fact, observed experimentally (Fig. 1*E*) at the OL/gradient interface, within the OL, and also within the iron sulfide–rich bands in the gradient region leading to the ML. This heterogeneous stress distribution therefore appears to provide an additional mechanism for energy dissipation in the most critical region of indentation via small localized regions of interfacial delamination while simultaneously preventing continuous and complete delamination of the entire OL from the ML or catastrophic fracture within the OL. The nanogranular substructure provides an even smaller level of waviness along the OL/ML, which results in advantageous smaller length scale heterogeneities in stresses and strains. It is interesting to see how *C. squamiferum* has created these additional different protection mechanism compared to other gastropod molluscs by using materials plentiful and specific to the deep-sea hydrothermal vent environment, i.e., vent fluids rich in dissolved sulfides and metals (2).

Thermal Simulations. *C. squamiferum* was found located at the base of the black smokers at the Kairei Field in a 1–2 m wide narrow transition zone where temperatures were measured in the range ≈2–10 °C (3). Deep sea hydrothermal vents are known to undergo drastic fluctuations in temperature due to emission of hot vent effluents (4). Hence, here we explore the resistance of the multilayered shell structure to a brief contact with a temperature of 100 °C (5). The thermal properties of OL, ML, CLL were taken as the values of greigite, that typical of organic biomacromolecules, and aragonite, respectively. A multilayered model (OL-ML-CLL, Fig. S4) was initially set to 2 °C. Then the outer surface was virtually heated up to 100 °C within 1 s, followed by a rapid cooling down to 2 °C within subsequent second (Fig. S4, dashed line). The maximum temperature on the inner surface (T_{inner}) in response to this transient pulse of extreme temperature was calculated to be 64 °C (Fig. S4). Interestingly, if the sequence of the ML and IL layers is reversed (OL-CLL-ML), a dramatic increase in T_{inner} is observed to 89.7 °C (Fig. S4) since the ML has higher thermal specific heat and lower thermal conductivity than the CLL. Placing the ML on the hotter side and IL on the colder side can enable the structure to exert maximum thermal protection. Lastly, a microlaminate structure approximating a nacreous microstructure was also simulated (Fig. S4) and, for this case, T_{inner} was observed to increase even further up to 91.7 °C. The apparent advantage of the multilayered structure of *C. squamiferum* over the microlaminate structure can be attributed to the high volume fraction of the organic phase characterized by low thermal conductivity and high heat capacity.

1. Shimizu S, Macho GA (2007) Functional significance of the microstructural detail of the primate dentino-enamel junction: A possible example of exaptation. *J Hum Evol*, 52(1):103–111.
2. Waren A, Bengtson S, Goffredi SK, Van Dover CL (2003) A hot-vent gastropod with iron sulfide dermal sclerites. *Science*, 302(5647):1007–1007.
3. Van Dover CL (2002) Trophic relationships among invertebrates at the Kairei hydrothermal vent field (Central Indian Ridge). *Mar Biol*, 141:761–772.
4. Van Dover CL, et al. (2001) Biogeography and ecological setting of Indian ocean hydrothermal vents. *Science*, 294:818–823.
5. McMullin ER, Bergquist DC, Fisher CR (2000) Metazoans in extreme environments: Adaptations of hydrothermal vent and hydrocarbon seep fauna. *Gravitational Space Biol Bull*, 13:13–23.

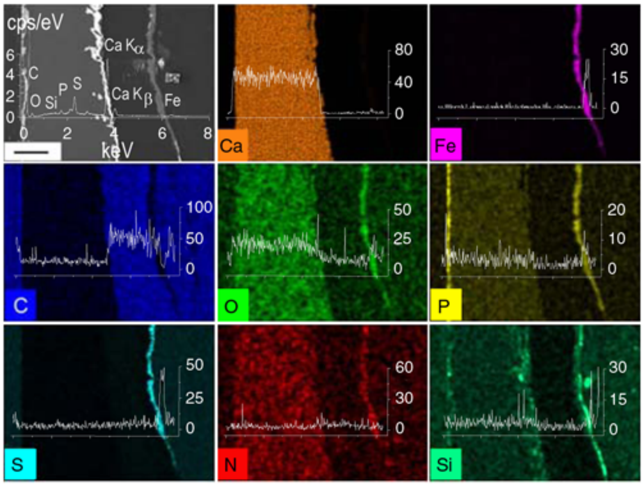

Fig. S1. EDX data on cross section of the *C. squamiferum* shell.

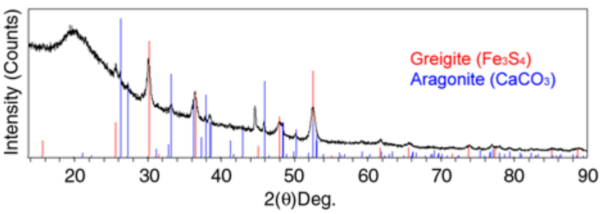

Fig. S2. X-ray diffraction of the *C. squamiferum* shell.

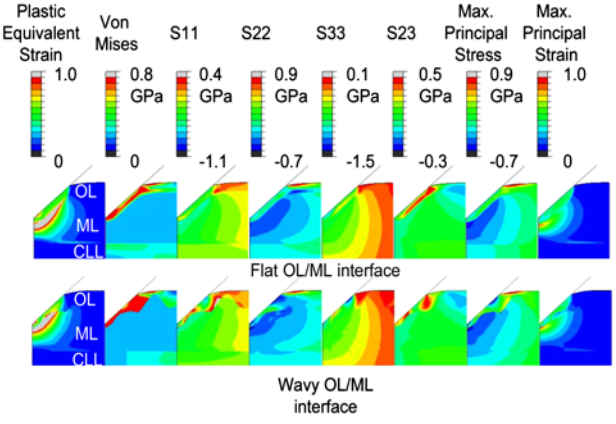

Fig. S3. Contours of predicted stress and strain for a wavy OL/ML interface compared to those for a flat OL/ML interface.

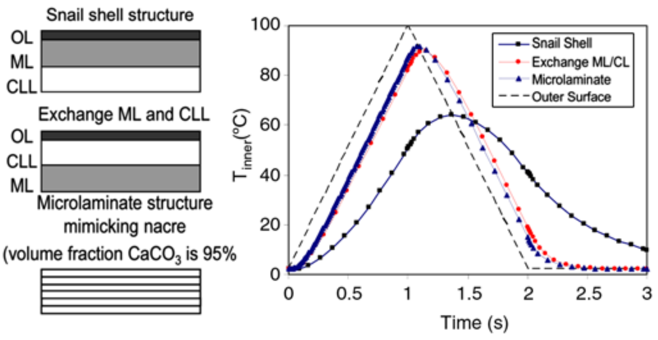

Fig. S4. Finite element simulation of resistance to thermal impulses of the *C. squamiferum* shell.